

MOND orbits in the Solar System's periphery and confrontation with the observations

L. Iorio

*INFN-Sezione di Pisa. Address for correspondence: Viale Unità di Italia 68
70125 Bari, Italy*

tel./fax 0039 080 5443144

e-mail: lorenzo.iorio@libero.it

Abstract

We look for MONDian orbital effects in the outer regions of the Solar System by numerically integrating both the MOND and the Newtonian equations of motions with the same initial conditions and investigate the resulting discrepancies. For the interpolating function μ of MOND we examine in details the “simple” form $\mu(X) = X/(1 + X)$. Major differences occur in the Oort cloud ($r \approx 50 - 150$ kAU) where highly elongated orbits are not allowed by MOND, contrary to Newtonian mechanics. This fact may have consequences on the composition and the dynamical history of the Oort cloud since the perturbations due to nearby passing stars, interstellar gas clouds and Galactic tides, which in the classical framework change the velocities of the Oort's comets launching them in the inner regions of the Solar System, would be less effective according to MOND. Then, we compare the predicted MOND heliocentric radial shifts Δr for some trans-Neptunian objects (Pluto and Sedna, $r \approx 40 - 500$ AU) and the giant gaseous planets Jupiter, Saturn, Uranus and Neptune ($r \approx 5 - 30$ AU) with the optical observations gathered during the last century. The MOND effects for Sedna are orders of magnitude smaller than the present-day orbit accuracy, while those for Pluto over 100 yr are about of the same order of magnitude, or even larger, of its orbit accuracy which will be improved when the New Horizon spacecraft will encounter Pluto in 2015. The MONDian departures Δr from the Newtonian paths over 80-100 yr for Neptune, Uranus, Saturn and Jupiter are, instead, quite larger than their orbit accuracy according to the latest DE (JPL, NASA), EPM (IAA, RAS) and INPOP (IMCCE) ephemerides in such a way that if $\mu = X/(1 + X)$ was valid as interpolating function also at acceleration scales of 10^5 in units of A_0 , its effects should have been detected.

Keywords: gravitation-ephemerides-methods: numerical

1 Introduction

In many astrophysical systems like, e.g., spiral galaxies and clusters of galaxies a discrepancy between the observed kinematics of their exterior parts and the predicted one on the basis of the Newtonian dynamics and the matter detected from the emitted electromagnetic radiation (visible stars and gas clouds) was present since the pioneering studies by Bosma [1] and Rubin and coworkers [2] on spiral galaxies. More precisely, such an effect shows up in the galactic velocity rotation curves whose typical pattern after a few kpc from the center differs from the Keplerian $1/\sqrt{r}$ fall-off expected from the usual dynamics applied to the electromagnetically-observed matter.

As a possible solution of this puzzle, the existence of non-baryonic, weakly-interacting Cold Dark (in the sense that its existence is indirectly inferred only from its gravitational action, not from emitted electromagnetic radiation) Matter (CDM) was proposed to reconcile the predictions with the observations [3] in the framework of the standard gravitational physics.

Oppositely, it was postulated that the Newtonian laws of gravitation have to be modified on certain acceleration scales to correctly account for the observed anomalous kinematics of such astrophysical systems without resorting to still undetected exotic forms of matter. One of the most phenomenologically successful modification of the inverse-square Newtonian law, mainly with respect to spiral galaxies, is the MODified Newtonian Dynamics (MOND) [4, 5, 6] which postulates that for systems experiencing total gravitational acceleration $A < A_0$, with [7]

$$A_0 = (1.2 \pm 0.27) \times 10^{-10} \text{ m s}^{-2}, \quad (1)$$

$$\mathbf{A} \rightarrow \mathbf{A}_{\text{MOND}} = -\frac{\sqrt{A_0 GM}}{r} \hat{\mathbf{r}}. \quad (2)$$

More precisely, it holds

$$A = \frac{N}{\mu(X)}, \quad X \equiv \frac{A}{A_0}; \quad (3)$$

$\mu(X) \rightarrow 1$ for $x \gg 1$, i.e. for large accelerations (with respect to A_0), while $\mu(X) \rightarrow x$ yielding eq. (2) for $x \ll 1$, i.e. for small accelerations. The most widely used forms for the interpolating function μ are

$$\mu(X) = \frac{X}{1+X}, \quad [8] \quad (4)$$

$$\mu(X) = \frac{X}{\sqrt{1+X^2}} \quad [9]. \quad (5)$$

It recently turned out that the simpler form of eq. (4) yields much better results in fitting the terminal velocity curve of the Milky Way, the rotation curve of the standard external galaxy NGC 3198 [8, 10, 11] and of a sample of 17 high surface brightness, early-type disc galaxies [12]. Eq. (38) strictly holds for co-planar, spherically and axially symmetric mass distributions [13]; otherwise, the full modified (non-relativistic) Poisson equation [9]

$$\nabla \cdot \left[\mu \left(\frac{|\nabla U|}{A_0} \right) \nabla U \right] = 4\pi G\rho, \quad (6)$$

where U is the gravitational potential, G is the Newtonian constant of gravitation and ρ is the matter density, must be used. See the Appendix for more detailed explanations. In the Solar System the aforementioned symmetry conditions holds, so that we will use eq. (38), as done by a number of other authors [4, 22, 23, 26].

Attempts to yield a physical foundation to MOND, especially in terms of a relativistic covariant theory, can be found in, e.g., [14, 15, 16]; for recent reviews of various aspects of the MOND paradigm, see [17, 18, 19].

In this paper we will numerically integrate both the MOND and the Newtonian equations of motion in different acceleration regimes by using the same initial conditions in order to look for departures of the MONDian trajectories with respect to the Newtonian ones. After setting the theoretical background which we will use in the rest of the paper (Section 2), we will explore the strong MONDian regime in the remote ($r = 50 - 150$ kAU) periphery of the Solar System, where the Oort cloud [20], populated by a huge number of small bodies moving along very eccentric and inclined to the ecliptic orbits, should exist (Section 3); for preliminary investigations on such a topic, see Ref. [4, 21]. In particular, we investigate the modifications that MOND would induce on the Newtonian orbits of a test particle moving in such a region; this will allow us to put forth some hypothesis on the overall configuration that the Oort cloud would have if MOND was valid. Then, we will move towards the inner regions of the Solar System populated by the trans-Neptunian objects (TNOs) where we will examine Sedna and Pluto (Section 4). Finally, we will look at the MONDian orbital effects on Neptune, Uranus, Saturn and Jupiter (Section 5). For other works on MOND in Solar System, see Ref. [4, 22, 23, 24, 25, 26]. In particular, the authors of Ref. [23] and Ref. [26] dealt with the weak limits of the interpolating functions of eq. (4) and eq. (5) by examining the corrections $\Delta\dot{\varpi}$ to the standard Newtonian/Einsteinian perihelion precessions of the inner planets recently estimated by E.V. Pitjeva in Ref. [27] in a purely phenomenological way by fitting about one century of data of various kinds with the dynamical

models of the EPM2004 ephemerides of the Institute of Applied Astronomy of the Russian Academy of Sciences. While the authors of Ref. [23] used one correction $\Delta\dot{\varpi}$ at a time for each planet by ruling out the (approximated) predictions for eq. (4), the author of Ref. [26] considered the ratios of the corrections $\Delta\dot{\varpi}$ for different pairs of planets by ruling out eq. (5) as well. Note that also Milgrom in Ref. [4] came to the same conclusions concerning eq. (4) as in [23, 26] by interpreting the results by Shapiro [28] concerning the Einsteinian perihelion precession of Mercury alone. Instead, Talmadge et al. [22] ruled out also eq. (5) by using Mercury and Mars. Since, at present, no other teams of astronomers have independently estimated their own corrections to the standard perihelion precessions by using the latest available observational dataset, in this paper we will not use the perihelia; instead, we will look at the heliocentric radius by also adopting the ephemerides DE by the Jet Propulsion Laboratory (JPL) of NASA and INPOP by the Institut de Mécanique Céleste et de Calcul des Éphémérides (IMCCE). The conclusions are in Section 6. In the Appendix we discuss the problem of the influence of the Galactic environment on the internal dynamics of the Solar System in MOND.

2 The MOND acceleration in the remote periphery of the Solar System

At heliocentric distances of 50-150 kAU the Newtonian acceleration due to the Sun is very weak amounting to only $2 \times 10^{-12} - 10^{-13} \text{ m s}^{-2}$, i.e. about $0.02A_0$; thus, it is, in principle, an ideal scenario to look for strong MONDian effects [4]. In the standard Newtonian framework, the Oort cloud is believed to be the reservoir of the long-period comets which are perturbed by nearby passing stars, Giant Molecular Clouds (GMCs) and Galactic tides [29] due to their highly elongated orbits. As a consequence of such interactions, temporary increases of the flux of comets entering the region of the planets—termed “comet showers”—may occur [30, 31]. MOND may change such a picture.

In dealing with the MOND dynamics of an Oort-type object, the so-called External-Field-Effect (EFE) [17, 19] must also be taken into account, in principle, according to

$$\mu\left(\frac{E+A}{A_0}\right)A=N, \quad (7)$$

where N is the Newtonian acceleration of the Sun-particle system alone, A

is the total internal acceleration of the system, while E denotes the gravitational acceleration induced by any field external to the system under examination. In fact, it can be shown that eq. (7) induces errors as small as $\approx 0.1\%$ with respect to [17, 19]

$$\mu \left(\frac{|\mathbf{A} + \mathbf{E}|}{A_0} \right) A = N. \quad (8)$$

See the Appendix for more details on EFE in the Solar System. By using the simpler form of eq. (4) for μ , one obtains

$$A = \frac{N}{2} \left[1 - \frac{E}{N} + \sqrt{\left(1 - \frac{E}{N}\right)^2 + \frac{4A_0}{N} \left(1 + \frac{E}{A_0}\right)} \right]. \quad (9)$$

For $A_0 \rightarrow 0$, $A \rightarrow N$, as expected. For $E \rightarrow 0$, i.e. $E \ll A_0$ and $E \ll N$, one has

$$A \rightarrow \frac{N}{2} \left(1 + \sqrt{1 + \frac{4A_0}{N}} \right). \quad (10)$$

For

$$\frac{E}{A_0} \ll 1, \quad (11)$$

the total acceleration becomes

$$A \approx \frac{N}{2} \left[1 - \frac{E}{N} + \sqrt{\left(1 - \frac{E}{N}\right)^2 + \frac{4A_0}{N}} \right], \quad (12)$$

while for

$$\frac{E}{N} \approx 1, \quad (13)$$

it is

$$A \approx \sqrt{NA_0} \left(1 + \frac{E}{A_0} \right). \quad (14)$$

Interestingly, if

$$\frac{E}{N} \approx 1, \quad \frac{E}{A_0} \ll 1, \quad (15)$$

then

$$A \approx \sqrt{NA_0} = \frac{\sqrt{GMA_0}}{r}. \quad (16)$$

Another case that may be relevant in certain circumstances is

$$E = A_0. \quad (17)$$

The total acceleration becomes

$$A = \frac{(N - E)}{2} \left[1 + \sqrt{1 + \frac{8A_0}{N \left(1 - \frac{A_0}{N}\right)^2}} \right]. \quad (18)$$

If

$$N \ll A_0, \quad (19)$$

as in the Oort cloud, then,

$$A \approx (N - E) \left(1 + \frac{2N}{A_0} \right) \approx N - E. \quad (20)$$

If

$$N \gg A_0, \quad (21)$$

as in the planetary regions of the Solar System, then

$$A \approx (N - E) \left(1 + \frac{2A_0}{N} \right) \approx N + E, \quad (22)$$

so that the external field can be treated with the standard perturbative techniques.

It must be stressed that, in MOND, the Galactic tides have not to be included in N , but in E . Here we will neglect the stochastic interactions with other stars and interstellar clouds. The Galactic tidal acceleration is approximately given by

$$T \approx \frac{GM_{\text{gal}}r}{R_{\odot}^3}, \quad (23)$$

where $R_{\odot} = 8.5$ kpc is the Galactocentric distance of the Sun, M_{gal} is the (baryonic) mass of the Milky Way and r is the heliocentric distance of an Oort-like object; it comes from the combination of the uniform centrifugal acceleration $C \approx A_0$ due to the overall circular motion of the Solar System as a whole through the Galaxy and the non-uniform gravitational attraction by the Galaxy. By assuming $M_{\text{gal}} = 10^{11}M_{\odot}$, it turns out

$$T \approx 10^{-15} - 10^{-14} \text{ m s}^{-2}, \quad r = 50 - 150 \text{ kAU}. \quad (24)$$

Its effect on the Oort cloud have been worked out in the framework of the Newtonian dynamics by several authors; see, e.g., Ref. [32] and references therein. Thus, eq. (10) seems a reasonable approximation, as we will explicitly show. Detailed explanations of the EFE in the Solar System can be found in the Appendix.

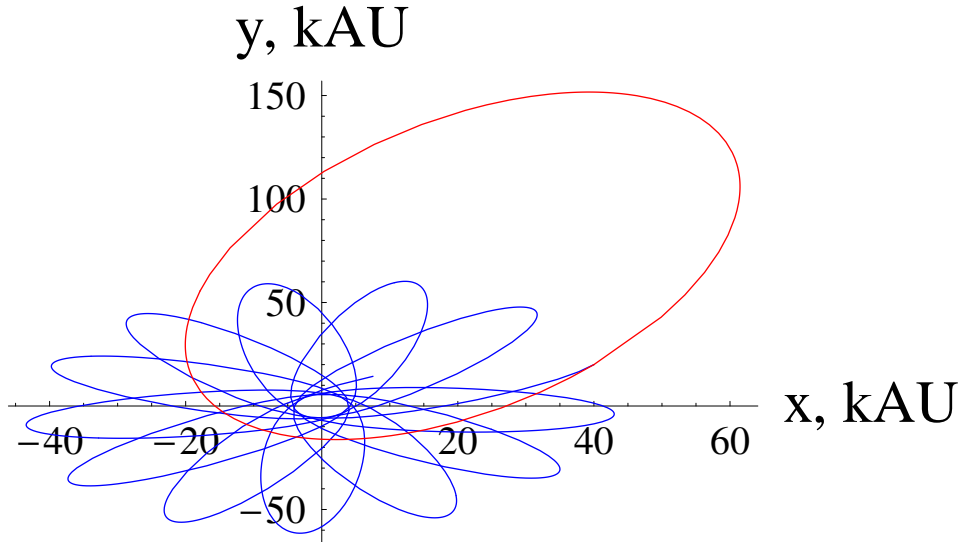


Figure 1: Sections in the $\{x, y\}$ plane of the numerically integrated trajectories of two Oort-type test particles around the Sun, located at the origin, affected by the MONDian acceleration of eq. (4) (blue line) and the Newtonian monopole $-GM/r^2$ (red line). For both particles it was assumed $x_0 = 40$ kAU, $y_0 = 20$ kAU, $z_0 = 38$ kAU, $\dot{x}_0 = -13$ kAU Myr $^{-1}$, $\dot{y}_0 = -25$ kAU Myr $^{-1}$, $\dot{z}_0 = -10$ kAU Myr $^{-1}$ (1 kAU Myr $^{-1} = 0.005$ km s $^{-1}$). They correspond to $i = 134$ deg, $a = 87.4$ kAU, $e = 0.82$. The integration interval correspond to the Keplerian orbital period $P_b = 26$ Myr.

3 Numerically integrated MOND orbits in the Oort cloud

In order to see how MOND modifies the Newtonian dynamics of an Oort-type object, we perform two numerical integrations of the equations of motion in cartesian coordinates according to MOND and the Newtonian dynamics sharing the same initial conditions corresponding to the standard Keplerian ellipse. We adopted adaptive algorithms automatically switching between BDF (Backward Differential Formulas) and Adams multistep methods depending on the stiffness of the equations.

In Figure 1-Figure 3 we show how a Keplerian ellipse with inclination to the ecliptic $i = 134$ deg, semimajor axis $a = 87.46$ kAU and eccentricity $e = 0.82$ would look like over a Keplerian orbital period $P_b = 26$ Myr if MOND was valid. In Figure 4-Figure 5 we plot the distance and the speed

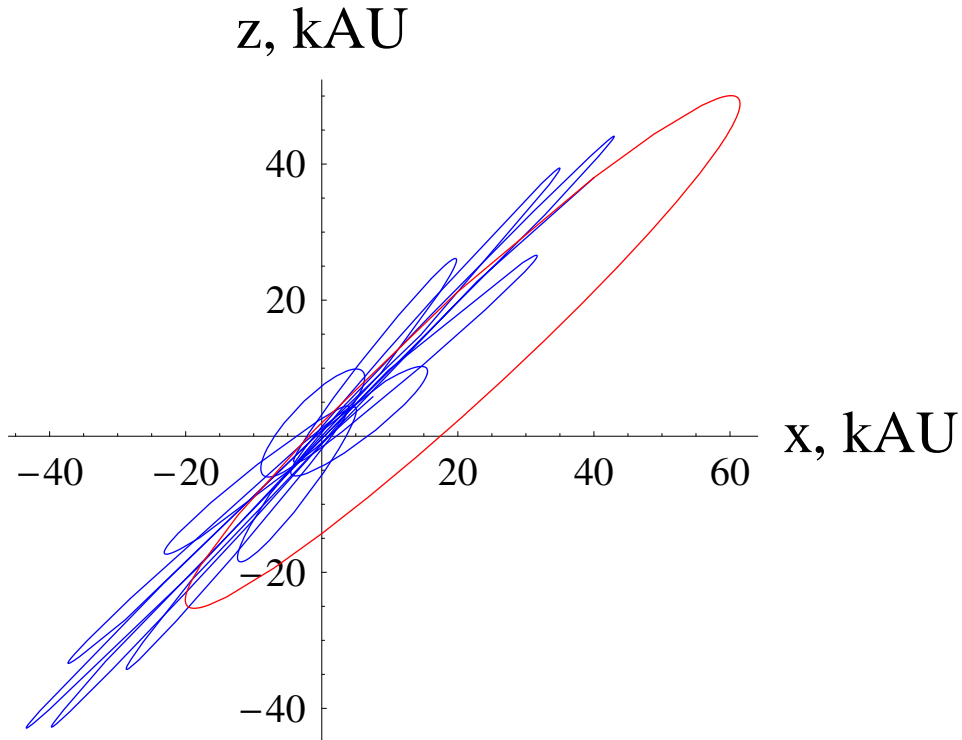


Figure 2: Sections in the $\{x, z\}$ plane of the numerically integrated trajectories of two Oort-type test particles around the Sun, located at the origin, affected by the MONDian acceleration of eq. (4) (blue line) and the Newtonian monopole $-GM/r^2$ (red line). For both particles it was assumed $x_0 = 40$ kAU, $y_0 = 20$ kAU, $z_0 = 38$ kAU, $\dot{x}_0 = -13$ kAU Myr $^{-1}$, $\dot{y}_0 = -25$ kAU Myr $^{-1}$, $\dot{z}_0 = -10$ kAU Myr $^{-1}$ (1 kAU Myr $^{-1} = 0.005$ km s $^{-1}$). They correspond to $i = 134$ deg, $a = 87.4$ kAU, $e = 0.82$. The integration interval correspond to the Keplerian orbital period $P_b = 26$ Myr.

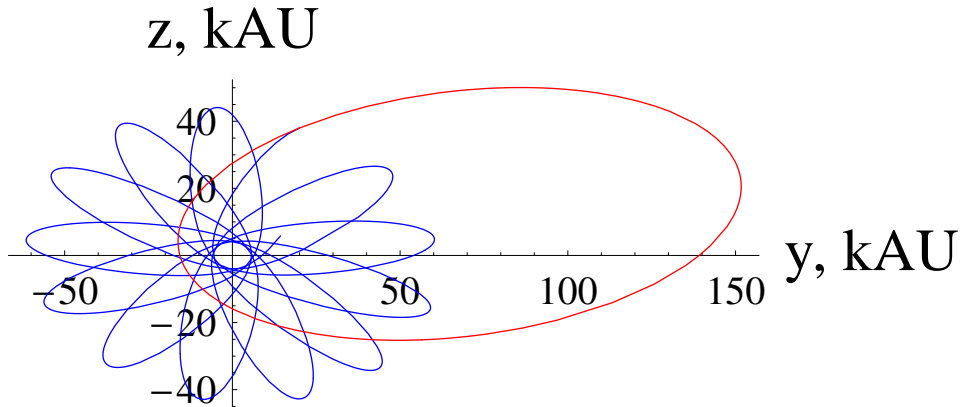


Figure 3: Sections in the $\{y, z\}$ plane of the numerically integrated trajectories of two Oort-type test particles around the Sun, located at the origin, affected by the MONDian acceleration of eq. (4) (blue line) and the Newtonian monopole $-GM/r^2$ (red line). For both particles it was assumed $x_0 = 40$ kAU, $y_0 = 20$ kAU, $z_0 = 38$ kAU, $\dot{x}_0 = -13$ kAU Myr $^{-1}$, $\dot{y}_0 = -25$ kAU Myr $^{-1}$, $\dot{z}_0 = -10$ kAU Myr $^{-1}$ (1 kAU Myr $^{-1} = 0.005$ km s $^{-1}$). They correspond to $i = 134$ deg, $a = 87.4$ kAU, $e = 0.82$. The integration interval correspond to the Keplerian orbital period $P_b = 26$ Myr.

as functions of time, while in Figure 6 we depict the speed as a function of the distance.

The orbit is still confined to a plane because of the conservation of the orbital angular momentum, but its shape and size are completely different. The minimum and, especially, the maximum heliocentric distances are quite smaller in MOND than in the Newtonian case; they are reached several times during one Keplerian orbital period (Figure 4). The speed attains almost always larger values in MOND than in Newtonian dynamics and it changes in time much frequently than in the Newtonian case (Figure 5). Moreover, v experiences a much more marked variation along the followed trajectory in MOND than in the Newtonian framework (Figure 6).

Such features may have consequences on the interaction of the Oort-like objects with passing stars [20] by reducing their perturbing effects and, thus, also altering the number of long-period comets launched into the inner regions of the Solar System, the number of comets left in the cloud throughout its history. Indeed, in the standard picture, the comets moving along very elongated orbits may come relatively close to a star of mass M_\star suffering a

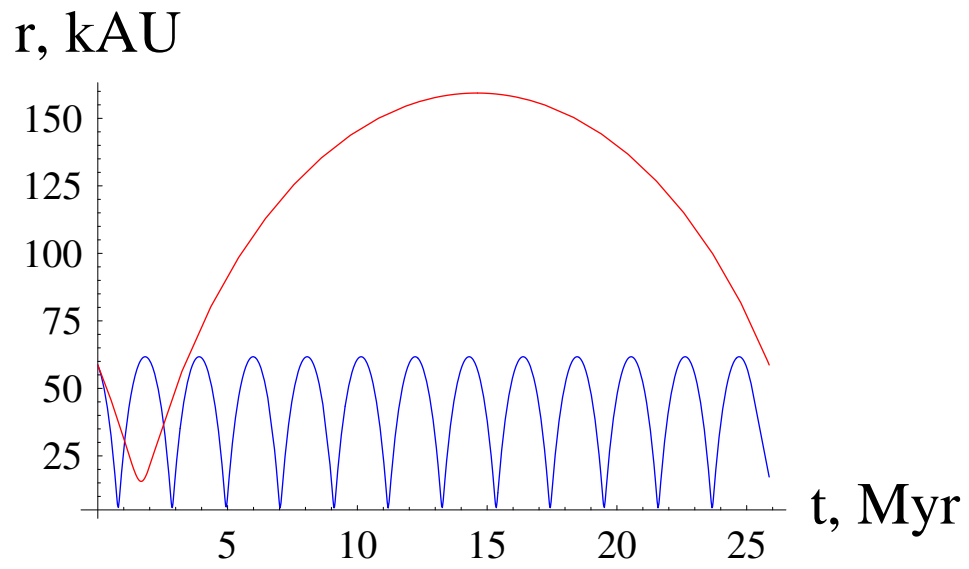


Figure 4: Blue line: heliocentric distance r (kAU) in MOND. Red line: heliocentric distance r (kAU) in Newtonian mechanics. The initial conditions and the integration interval are those of Figure 1-Figure 3.

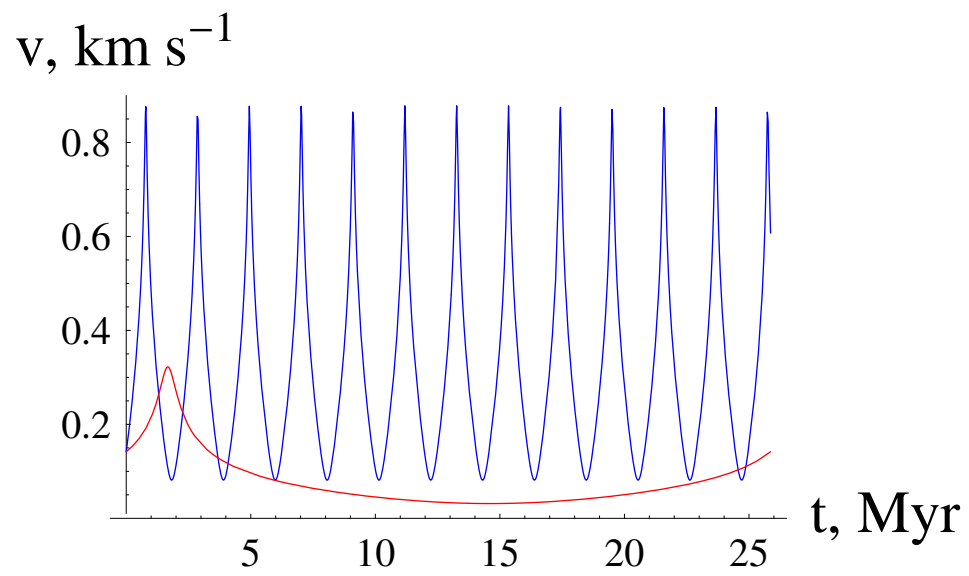


Figure 5: Blue line: speed v (km s^{-1}) in MOND. Red line: speed v (km s^{-1}) in Newtonian mechanics. The initial conditions and the integration interval are those of Figure 1-Figure 3.

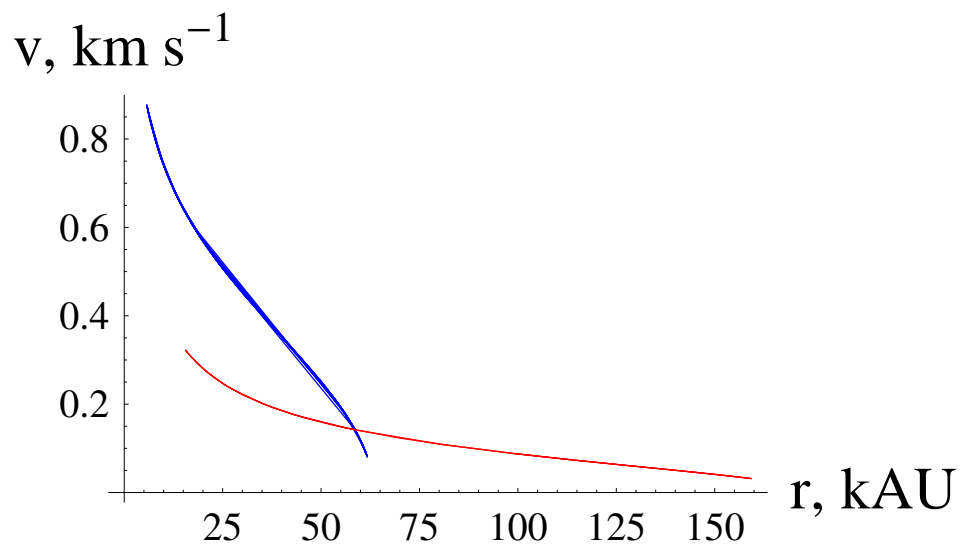


Figure 6: Blue line: speed v (km s^{-1}) in MOND. Red line: speed v (km s^{-1}) in Newtonian mechanics. The distance r is in kAU . The initial conditions are those of Figure 1-Figure 3.

change in velocity Δv which approximately is [20]

$$\Delta v = \frac{2GM_\star}{v_\star d}, \quad (25)$$

where v_\star is the star's velocity with respect to the Sun and d is the distance of closest approach with the Oort object. Moreover, less elongated orbits would also reduce the perturbing effects of the Galactic tides.

4 The trans-Neptunian objects

Let us, now examine the possibility of direct testing MOND by examining the orbital motions of some bodies in the closer periphery of the Solar System ($r \gtrsim 0.03$ kAU). At first sight, such an idea may seem bizarre because MONDian departures from the usual Newtonian dynamics are expected to be negligible in such region where $N/A_0 \approx 10^4$, but, as we will see, they might be not excessively small with respect to the present-day level of accuracy in determining the orbital motions in the inner region of the TNOs field, at least for some selected bodies. In this Section we will straightforwardly use eq. (4) since the Galactic tidal effects are completely negligible with respect to both N and A_0 . In Figure 60 we plot the difference between the heliocentric distances of 134340 Pluto ($a = 39.5$ AU, $e = 0.24$, $i = 17.2$ deg), for which available observations since January 1914 exist, from two numerically integrated Newtonian and MONDian trajectories sharing the same initial conditions corresponding to 23 April 1965 retrieved from the HORIZONS system by NASA (<http://ssd.jpl.nasa.gov/?horizons>). MONDian deviations Δr from the Newtonian trajectory amount to about 20-200 Mm (1 Mm = 10^6 m) over 100 yr. Such values can be compared with the latest determinations of the Pluto's orbital elements. Since the average heliocentric distance is

$$\langle r \rangle = a \left(1 + \frac{e^2}{2} \right), \quad (26)$$

its uncertainty can conservatively be evaluated as

$$\delta \langle r \rangle \leq \delta a \left(1 + \frac{e^2}{2} \right) + ae\delta e. \quad (27)$$

According to Table 3 of [34], obtained with the EPM2006 ephemerides by E. V. Pitjeva, the formal, statistical uncertainty in a amounts to

$$\delta a = 34.1 \text{ Mm}, \quad (28)$$

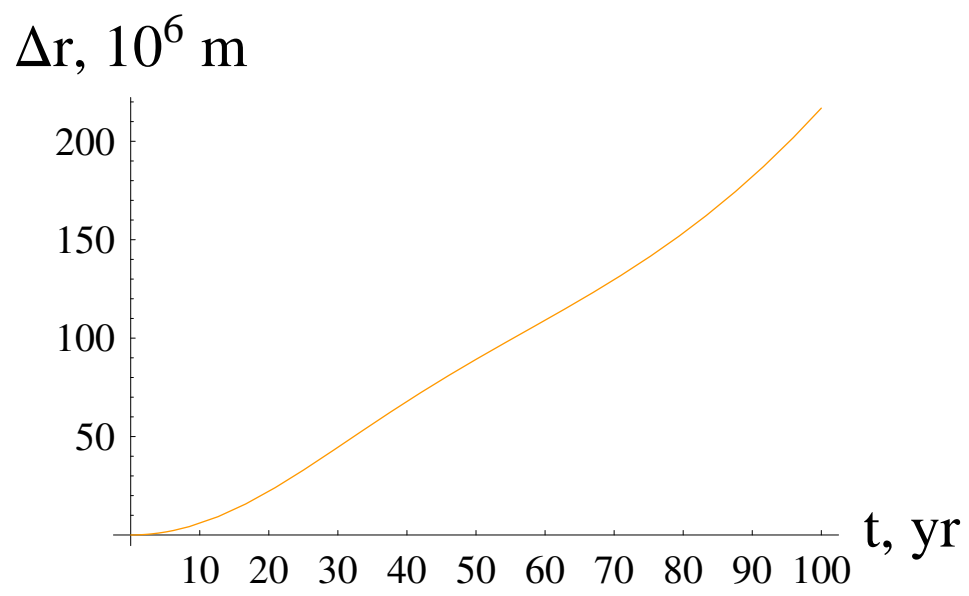


Figure 7: Difference Δr over 100 yr between the heliocentric distances of Pluto from two numerically integrated Newtonian and MONDian trajectories sharing the same initial conditions retrieved from the HORIZONS system by NASA.

while the uncertainty in the eccentricity e can be obtained from the non-singular elements $h = e \cos \varpi$ and $k = e \sin \varpi$ as

$$\delta e \leq \frac{|h|\delta h + |k|\delta k}{e} = 2 \times 10^{-6}. \quad (29)$$

Thus, the uncertainty in the average heliocentric distance of Pluto is

$$\delta \langle r \rangle_{\text{Pluto}} \lesssim 59.5 \text{ Mm}. \quad (30)$$

The result of eq. (30) tells us that the predicted MONDian departures from the Newtonian orbit of Pluto after about 30 yr would be measurable; thus, it might be argued that, since no deviations from the usual Newtonian behavior as large as those predicted by MOND have been so far detected in the Pluto's data, MOND would be in trouble. However, caution is in order because it must be noted that eq. (30) has been obtained by taking the $1 - \sigma$ formal uncertainties; since only relatively inaccurate optical data are available so far for Pluto, the realistic error in its orbit may be, very conservatively, up to 10 times larger. On the other hand, according to Fig. 14 by Folkner et al. [35], the uncertainty in the Pluto heliocentric distance, evaluated as the difference between the DE418 and DE414 ephemerides from 1900 to 2020, may be up to 20 Mm. Smaller figures, of the order of 1 – 5 Mm, are quoted in Figure 15 and Figure 16 of Ref. [35] in which the interval 1920-2020 is considered. The difference between the DE405 and INPOP06 ephemerides over 100 yr quoted in Table 4, 2nd column, of Ref. [36] yields an uncertainty in the heliocentric range of Pluto of 35 Mm. By the way, the situation may change in the near future because Pluto is the target of the spacecraft-based New Horizons mission which should greatly improve, among other things, also our knowledge of the orbit of Pluto, to be reached in 2015.

It maybe interesting to look also at 90377 Sedna (2003 VB12) ($a = 514$ AU, $e = 0.85$, $i = 11.9$ deg), for which available observations since September 1990 exist, to have an idea of what could be the perspectives in using it for testing MOND; after all, the MONDian effects on Sedna should be larger than on Pluto. By proceeding as for Pluto, we see in Figure 8 that the MONDian departures Δr from the Newtonian trajectory amount to about 0.0005 – 0.003 AU over 100 yr, while

$$\delta \langle r \rangle_{\text{Sedna}} \lesssim 3.3 \text{ AU}, \quad (31)$$

where we used the formal $1 - \sigma$ uncertainties $\delta a = 2.2203$ AU, $\delta e = 0.00070246$ retrieved from the JPL Small-Body Database Browser (<http://ssd.jpl.nasa.gov/sbdb.cgi>).

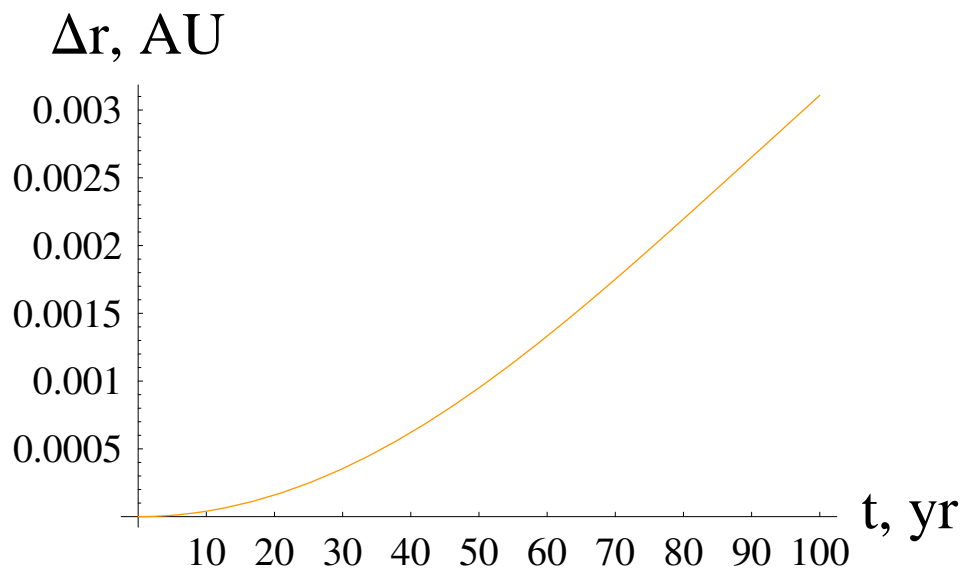


Figure 8: Difference Δr over 100 yr between the heliocentric distances of Sedna from two numerically integrated Newtonian and MONDian trajectories sharing the same initial conditions retrieved from the HORIZONS system by NASA.

In this case, the MOND-induced shift of Sedna is 3 – 4 orders of magnitude smaller than the present-day accuracy in knowing its orbit.

Summarizing this Section, Sedna is the body which, in principle, exhibits the largest MONDian orbital effects among the trans-Neptunian objects, but the present-day accuracy in knowing its orbit is too poor by 3 – 4 orders of magnitude to appreciate them. The case of Pluto is more interesting because the MONDian effects on its path are about of the same order of magnitude, or even larger, of its orbital accuracy which should be improved in the mid future thanks to the New Horizon mission. By the way, the present-day situation for Pluto does not allow to infer a firm conclusion about its MONDian effects.

5 The giant gaseous planets

Leaving the TNOs to move towards the region of the giant gaseous planets, it turns out that the MOND trajectory of Neptune ($a = 30$ AU, $e = 0.008$, $i = 1.8$ deg) deviates from the Newtonian one by $\Delta r \approx 20 - 150$ Mm over 100 yr, as depicted by Figure 9. Quite interestingly, the numerous optical observations for Neptune processed by Pitjeva [34] yield

$$\delta \langle r \rangle_{\text{Neptune}} \leq 0.8 \text{ Mm}, \quad (32)$$

where we used the formal $1 - \sigma$ uncertainties [34] $\delta a = 0.46$ Mm, $\delta e = 0.0000105326$. In this case, even by re-scaling them by a factor 10, the MOND effect should have not escaped from detection if it existed. Another way to deal with the problem of assessing the realistic accuracy in knowing Neptune’s orbit from optical data is as follows. The latest Charge Coupled Device (CCD)-based observations of the outer planets are accurate to about [34] 0.06 arcsec level; this translates into an about 1 – 1.6 Mm accuracy at Neptune’s distance which becomes about 4 Mm if one considers the ≈ 0.2 arcsec accuracy of the older photographic observations. The confrontation between the DE410 and DE405 ephemerides from 1970 to 2010 in Fig. 2 of Ref. [37] yields an uncertainty up to about 1 Mm. Table 4, 2nd column, in Ref. [36] yields 3.2 Mm for the uncertainty in the Neptune’s heliocentric distance over 100 yr evaluated as difference between the DE405 and INPOP06 ephemerides. Thus, MOND seems seriously challenged by Neptune.

The situation for Uranus ($a = 19$ AU, $e = 0.046$, $i = 0.77$ deg), whose MOND discrepancy from the Newtonian case over 100 yr is shown in Figure 10, is even more neat. Indeed, its maximum value is of the order of 40 Mm, while Table 3 of Ref. [34] yield for the formal $1 - \sigma$ errors $\delta a = 0.04$ Mm

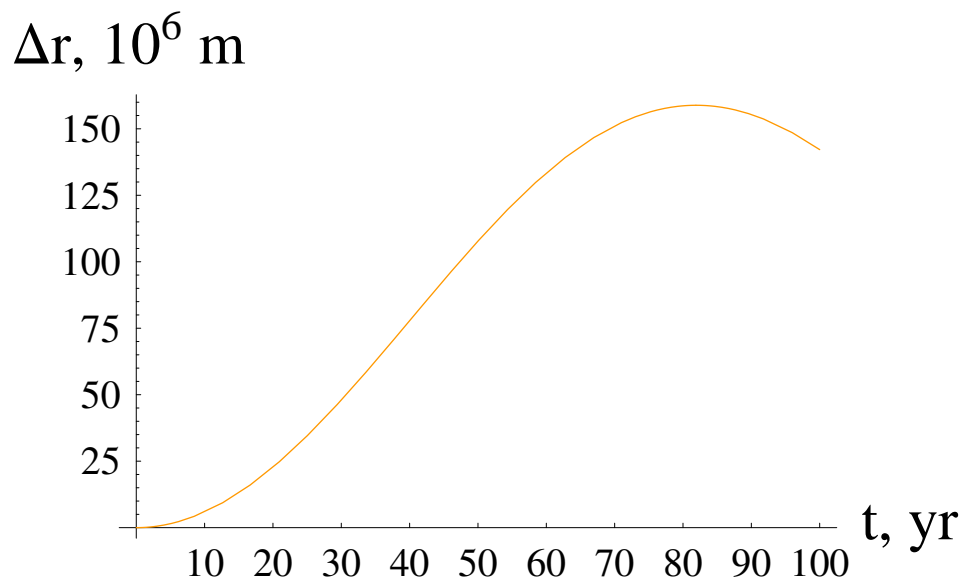


Figure 9: Difference Δr over 100 yr between the heliocentric distances of Neptune from two numerically integrated Newtonian and MONDian trajectories sharing the same initial conditions retrieved from the HORIZONS system by NASA.

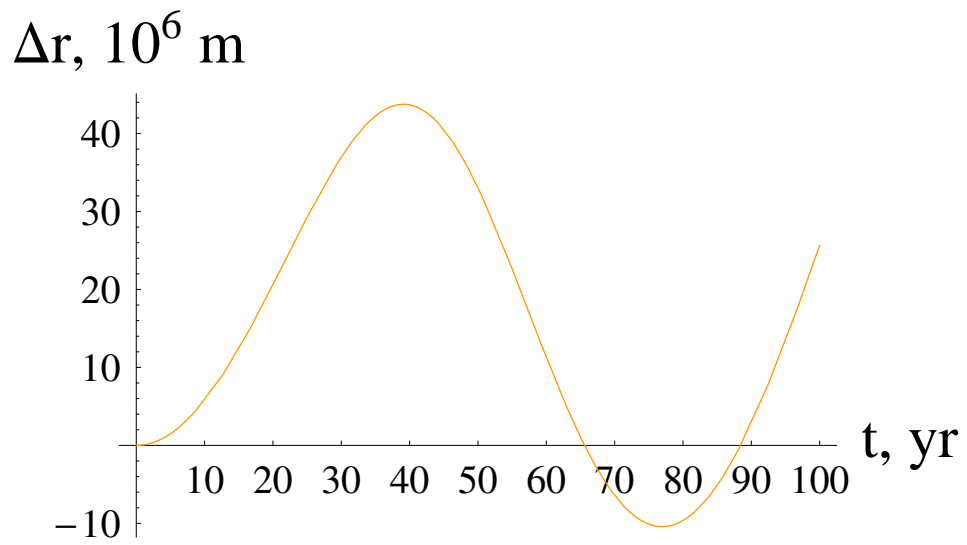


Figure 10: Difference Δr over 100 yr between the heliocentric distances of Uranus from two numerically integrated Newtonian and MONDian trajectories sharing the same initial conditions retrieved from the HORIZONS system by NASA.

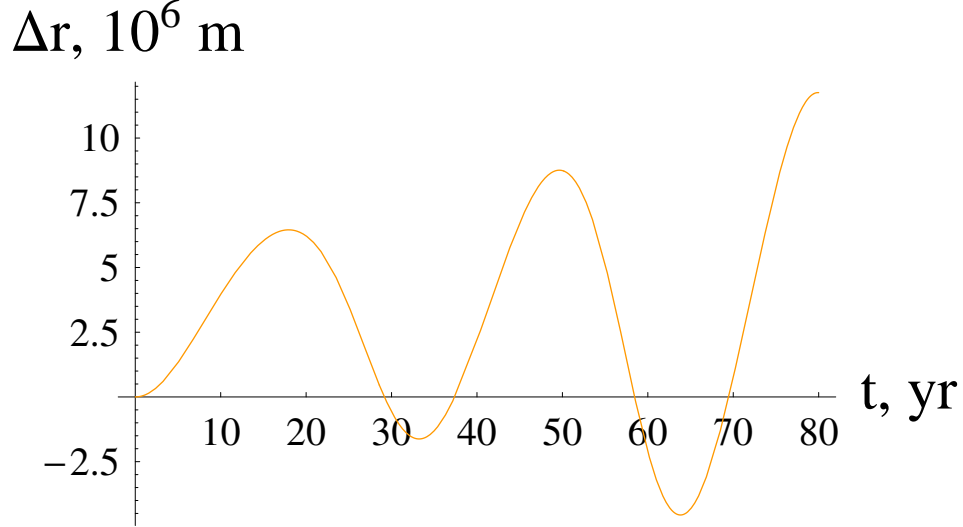


Figure 11: Difference Δr over 80 yr between the heliocentric distances of Saturn from two numerically integrated Newtonian and MONDian trajectories sharing the same initial conditions retrieved from the HORIZONS system by NASA.

and $\delta e = 4 \times 10^{-7}$, so that

$$\delta \langle r \rangle_{\text{Uranus}} \leq 0.1 \text{ Mm}. \quad (33)$$

By re-scaling it by a factor 10 or, equivalently, by mapping the angular error of 0.1 arcsec into a radial uncertainty at the Uranus' distance, one gets about 1 Mm. The same result is also obtained in Figure 2 of Ref. [37] by comparing the DE410 and DE405 ephemerides from 1970 to 2010, and in 2nd column of Table 4 in Ref. [36] by taking the difference over 100 yr between the DE405 and INPOP06 ephemerides. Such a level of accuracy is good enough to have allowed for the detection of the MOND effects on Uranus.

The MONDian behavior of Saturn ($a = 9.5 \text{ AU}$, $e = 0.055$, $i = 2.5 \text{ deg}$) with respect to the Newtonian one over 80 yr is depicted in Figure 11. The discrepancy lies in the range 1 – 10 Mm, while Table 3 of Ref. [34], in which only optical data have been used, yields the formal $1 - \sigma$ errors $\delta a = 4256 \text{ m}$, $\delta e = 4 \times 10^{-7}$, so that

$$\delta \langle r \rangle_{\text{Saturn}} \leq 0.04 \text{ Mm}. \quad (34)$$

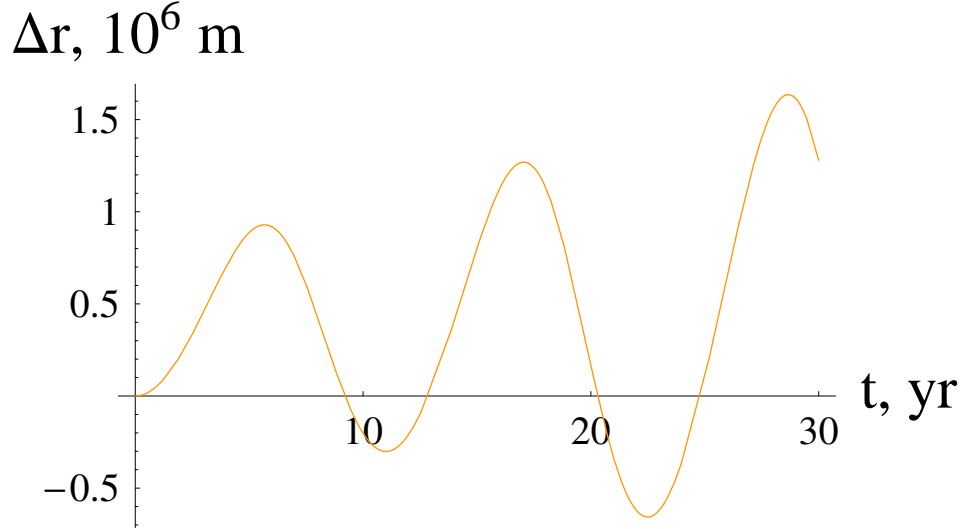


Figure 12: Difference Δr over 80 yr between the heliocentric distances of Jupiter from two numerically integrated Newtonian and MONDian trajectories sharing the same initial conditions retrieved from the HORIZONS system by NASA.

Figure 2 of Ref. [37], obtained by comparing the DE410 and DE405 ephemerides from 1970 to 2010, yields a maximum uncertainty of 0.2 Mm. Table 4, 2nd column of Ref. [36] yields an uncertainty of 0.29 Mm in the heliocentric distance of Saturn by taking the difference between the DE405 and INPOP06 ephemerides over 100 yr.

The case of Jupiter ($a = 5.2 \text{ AU}$, $e = 0.048$, $i = 1.3 \text{ deg}$), for which also radiometric observations from several spacecrafts (Pioneer 10-11, Voyager, Ulysses, Galileo) have been used in, e.g., [34], is shown in Figure 12. The MOND effect lies in the range 0.1-1.5 Mm over 30 yr, while the formal $1 - \sigma$ errors in a and e in Table 3 of [34] yield

$$\delta \langle r \rangle_{\text{Jupiter}} \leq 0.002 \text{ Mm}. \quad (35)$$

Fig. 2 of Ref. [37] shows the difference between the DE410 and DE405 ephemerides from 1970 to 2010; the maximum uncertainty in r is about 0.02 Mm. The uncertainty in r , evaluated as difference between the DE405 and INPOP06 ephemerides over 100 yr, quoted in Table 4, 2nd column of [36] amounts to 0.03 Mm.

In principle, one should also include the mutual N -body interactions

between all the major bodies of the Solar System in N when both the MONDian and the Newtonian equations of motion are integrated, but it is unlikely that they can substantially alter the results obtained so far.

It might be argued that, since MOND was not modelled in the ephemerides considered, the fact that its predicted effects do not show up in the observed planetary motions may be due to some sort of total/partial “absorption” of the MONDian effects in the estimation of the planets’ initial state vectors; as a consequence, one should explicitly model MOND and estimate, among other things, a dedicated parameter explicitly accounting for it. On the other hand, it could be argued that the size of the predicted MOND effects is so large that such a simultaneous removal of its signature from all the planets’ determined orbits seems unlikely.

In summary, the accuracy in our knowledge of the orbits of Neptune, Uranus, Saturn and Jupiter is good enough to having allowed for a detection of the relatively large MOND effects, for $\mu(X) = X/(1 + X)$, on their trajectories.

We mention that repeating the previous analysis with the standard form $\mu(X) = X/\sqrt{1 + X^2}$, it turns out that the discrepancies between the Newtonian and MONDian trajectories are too small to have been detected in the motions of the outer planets of the Solar System.

6 Summary and conclusions

We have numerically investigated the orbital motions of test particles according to MOND in different regions of the Solar System: the Oort cloud ($r \approx 50 - 150$ kAU), the mid-inner Kuiper belt ($r \approx 40 - 500$ AU) and the outer region of the gaseous giant planets ($r \approx 5 - 30$ AU). As MONDian interpolating function $\mu(X)$, we extensively used the form $\mu(X) = X/(1 + X)$ which recently turned out to yield better results in the galaxies realm than the older one $\mu = X/\sqrt{1 + X^2}$. We integrated both the MOND and the Newtonian equations of motion in Cartesian coordinates sharing the same initial conditions retrieved with the HORIZONS software by NASA and compared the resulting orbital trajectories; for Jupiter, Saturn, Uranus, Neptune, Pluto and Sedna we also computed the difference Δr between the resulting heliocentric distances over 100 yr.

The structure and the dynamical history of the Oort cloud, in deep MONDian regime, would be altered with respect to the standard Newtonian picture because highly eccentric orbits would not be allowed by MOND which, on the contrary, strongly tends to shrink them. As a consequence,

one may speculate that the number of long-period comets launched in the inner parts of the Solar System should be reduced because of the less effective perturbing actions of nearby passing stars, interstellar clouds and Galactic tides.

In the Kuiper belt, Sedna exhibits MOND departures from the standard Newtonian picture which are orders of magnitude smaller than the present-day accuracy in determining its orbit. The situation for Pluto is more favorable because the MOND effects on it over one century are about of the same order of magnitude, or even larger, of its orbital accuracy. Moreover, it should be improved by the ongoing New Horizons mission which should reach Pluto in 2015.

Concerning Neptune, Uranus, Saturn and Jupiter their MONDian departures from the Newtonian paths over a time span of 80-100 yr, computed by neglecting in N the \mathcal{N} -body mutual interactions with the other major bodies of the Solar System, are, in fact, 1 order of magnitude, or even more, larger than the realistic accuracy in determining their orbits from modern optical observations processed with various ephemerides produced by different institutions (EPM by Institute of Applied Astronomy of the Russian Academy of Sciences, DE by Jet Propulsion Laboratory of NASA, INPOP by Institut de Mécanique Céleste et de Calcul des Éphémérides) over just one century. Since such effects have not been detected so far, this poses a further serious challenge to the validity of the MONDian interpolating function used here, in the Solar System, in agreement with the results obtained in previous studies by using the corrections $\Delta\dot{\omega}$ to the standard Newtonian/Einsteinian perihelion precessions estimated by E.V. Pitjeva with the EPM ephemerides and by other researchers using older datasets processed with different ephemerides. In principle, there is the possibility that the MONDian signatures, not modelled in the ephemerides used to process the data, may have been totally/partially removed in the estimation process of the planetary initial conditions; on the other hand, it may be noted that the size of the MOND effects is so large that it is unlikely that such an uniform removal from all the planets' determined orbits may have occurred. Anyway, a complementary test that could be done may consist in explicitly modeling MOND in the dynamical force models of the ephemerides and estimating, among other things, an ad-hoc, dedicated parameter accounting for it.

We mention that $\mu(X) = X/\sqrt{1+X^2}$ survives the test presented here.

Finally, we wish to note that the analysis presented here does, in fact, not represent a test of MOND itself, but of the interpolating function used. Since it is not inferred from basic principles but just phenomenologically, it seems more appropriate to conclude that the slope of the interpolating

function must display a new change at large accelerations. Indeed, it is not possible, in principle, to assume that the analytical form derived by Famaey and Binney for $\mu(X)$ at galactic scales should be applicable at an acceleration range of 10^5 in units of A_0 .

Appendix. The External Field Effect in the Solar System

In the framework of their (non-relativistic) Lagrangian-derived theory of MOND, Bekenstein and Milgrom in Ref. [9] proposed the following form of a modified Poisson equation

$$\nabla \cdot \left[\mu \left(\frac{|\nabla U|}{A_0} \right) \nabla U \right] = 4\pi G\rho, \quad (36)$$

where $-\nabla U = \mathbf{A}$ is the internal acceleration of the system s considered, $\mu(X)$ is identified with the MONDian interpolating function. For simple uni-dimensional symmetries (spherical, cylindrical and planar) it exactly holds [38, 13]

$$\mu \left(\frac{A}{A_0} \right) \mathbf{A} = \mathbf{N}, \quad (37)$$

where $A = |\mathbf{A}|$ and $\mathbf{N} = -\nabla U_N$ is the Newtonian internal acceleration of s which, in our case, is the Solar System for which such symmetries are certainly satisfied. In fact, by applying the usual Poisson equation to the right-hand side of eq. (36), i.e., $\nabla \cdot \nabla U_N = 4\pi G\rho$, it can be obtained that eq. (37) is valid up to a $\nabla \times \mathbf{h}$ term in its right-hand-side: for the above-mentioned symmetries the curl term is identically zero.

In order to empirically account for the fact that in certain open globular clusters in the Galactic neighborhood of the Sun no large mass discrepancy was found, although the internal accelerations are smaller than A_0 , it was postulated that also the external field \mathbf{E} due to a larger system S in which s is assumed to be embedded plays a determinant role in MOND [4, 38]. The theoretical status of such a feature is still unclear [17, 19] in the sense that it is currently uncertain if it can be considered as a general consequence of the premises alone, i.e. a genuine prediction or just a phenomenological request; it has been implemented in several ways in all versions of MOND studied to date. In a very common version of EFE [17, 39, 40] eq. (37) approximately becomes

$$\mu \left(\frac{|\mathbf{A} + \mathbf{E}|}{A_0} \right) \mathbf{A} \approx \mathbf{N}. \quad (38)$$

Eq. (38) is only an approximate and effective way to take into account the effect of the external field on local physics, in order to avoid solving the modified Poisson equation by Bekenstein and Milgrom [9] with an external source term ρ_{ext} on the right-hand side [39]. In our case S will be the Milky Way in which the Solar System moves describing an approximately circular orbit with a period of about 230 Myr.

It can be noted that the direction of \mathbf{A} is that of \mathbf{N} , i.e.

$$\frac{\mathbf{A}}{A} = \frac{\mathbf{N}}{N}, \quad (39)$$

while the magnitude A of the internal acceleration is different from the Newtonian one N ; more precisely, A is larger than N by an amount which cannot be much larger than A_0 since MOND mainly differs from Newtonian mechanics just when the internal acceleration is of the same order of, or smaller than A_0 [41]. Concerning the interpolating function μ , we will use for it both the “simple” form [8] which, apart from being well tractable, yields good results in fitting the rotation curves of the Milky Way and of other galaxies, and the “standard” one [9]. Instead of using

$$X \equiv \frac{|\mathbf{A} + \mathbf{E}|}{A_0} = \frac{\sqrt{A^2 + E^2 + 2AE \cos \alpha}}{A_0}, \quad (40)$$

where $E = |\mathbf{E}|$ and α is the angle between \mathbf{A} and \mathbf{E} , we will use

$$X \equiv \frac{A + E}{A_0} \quad (41)$$

by discussing later the validity of such an useful approximation.

Let us, first, start with eq. (4). From eq. (38), with eq. (4) and eq. (41), it is possible to obtain

$$A = \frac{N}{2} \left[\left(1 - \frac{E}{N}\right) + \sqrt{\left(1 - \frac{E}{N}\right)^2 + \frac{4A_0}{N} \left(1 + \frac{E}{A_0}\right)} \right]. \quad (42)$$

The question now arises: what kind of external field has to be included into \mathbf{E} ? Such an issue, in my opinion, has never been treated with a sufficient level of clarity, especially from the point of view of the underlying assumptions concerning the reference frames to be used. Let us assume a step-by-step, phenomenological approach. It seems that, with the formulation of EFE followed here, \mathbf{E} should be the one due to the free-fall of the

Solar System through the Milky Way which can be obtained from its centrifugal acceleration; for $R_{\odot} = 8.5$ kpc and $v_{\odot} = 220$ km s⁻¹, it amounts to $C = 1.8 \times 10^{-10}$ m s⁻², i.e. $C \approx A_0$. If MOND was a linear theory of gravity, \mathbf{C} would not play any role in the internal dynamics of the Solar System because it would equally affect both the Sun and the planets in their motion through the Galaxy, so that it would cancel when the relative Sun-planet motion is considered. Our eq. (42), which just yield the acceleration of a test particle with respect to a body of mass M , fulfils such a condition: indeed, for $A_0 \rightarrow 0$, one has that $A \rightarrow N$, as expected: in the limit of vanishing A_0 , the usual Newtonian mechanics, without EFE, is restored.

Let us, now, assume $\mathbf{C} = \mathbf{E}$ and see what are the consequences of such a choice in MOND according, first, to eq. (42). For $E = A_0$, it becomes

$$A = \frac{N}{2} \left[\left(1 - \frac{E}{N}\right) + \left|1 - \frac{E}{N}\right| \sqrt{1 + \frac{8E}{N \left(1 - \frac{E}{N}\right)^2}} \right], \quad (43)$$

where we used

$$\left|1 - \frac{E}{N}\right| = \sqrt{\left(1 - \frac{E}{N}\right)^2}. \quad (44)$$

Let us, now look at the following limiting cases.

- The internal Newtonian acceleration N is quite smaller than the external acceleration E , assumed equal to A_0 . This fact ($N \ll A_0$) happens, e.g., in the Oort cloud. In this case,

$$\frac{E}{N} \gg 1, \quad (45)$$

so that

$$\left|1 - \frac{E}{N}\right| = -\left(1 - \frac{E}{N}\right). \quad (46)$$

Thus,

$$A \approx 2N \left(1 - \frac{N}{E}\right) \approx 2N; \quad (47)$$

the internal dynamics is almost Newtonian, as expected in the cases in which $A \ll A_0 \lesssim E$ [4, 38, 17]. In this case, $\Delta \equiv A - N = N \left(1 - \frac{2N}{E}\right) \approx N$ which is smaller than A_0 .

- The internal Newtonian acceleration N is quite larger than the putative external acceleration E , assumed equal to A_0 : this fact ($N \gg A_0$)

happens, e.g., in the planetary regions of the Solar System. In this case,

$$\frac{E}{N} \ll 1, \quad (48)$$

so that

$$\left|1 - \frac{E}{N}\right| = \left(1 - \frac{E}{N}\right). \quad (49)$$

Thus,

$$A \approx (N - E) \left(1 + \frac{2E}{N}\right) \approx N + E. \quad (50)$$

In this case, $\Delta \equiv A - N = E$, which is just equal to A_0 . Note also that, for $r \rightarrow \infty$, $\mathbf{A} \rightarrow \mathbf{E}$. Note that such a result would hold also if one used [42]

$$\mu \left(\frac{|\mathbf{A} + \mathbf{E}|}{A_0}\right) (\mathbf{A} + \mathbf{E}) = \mathbf{N} \quad (51)$$

instead of eq. (38).

Let us, now, examine the consequences of eq. (50). It tells us that, in MOND, an external field E as large as A_0 does affect the dynamics of a test particle also in the weak MONDian regime. This fact yields to a contradiction with the planetary observations. Indeed, since

$$\mathbf{A} = A \frac{\mathbf{N}}{N} = (N + E) \frac{\mathbf{N}}{N} = \left(-\frac{GM}{r^2} + E\right) \frac{\mathbf{r}}{r}, \quad (52)$$

\mathbf{E} can be treated with the standard perturbative techniques as a small radial perturbation of the Newtonian monopole yielding an anomalous secular perihelion precession [23, 25, 43]

$$\dot{\omega}_C = E \sqrt{\frac{a(1 - e^2)}{GM}}, \quad (53)$$

where a and e are the semimajor axis and the eccentricity of the planetary orbit. Table 1 tells us that such an effect, for $E = C = A_0 \propto 10^{-10} \text{ m s}^{-2}$, would have been too large to have escaped detection.

Concerning the validity of our approximation of eq. (41), it is well justified. Indeed, it turns out that, in the case of $N/E \gg 1$, the values of μ computed with eq. (41) for a typical Solar System planetary orbit ($a = 30 \text{ AU}$) differ from those computed as a function of $0 \leq \alpha \leq 2\pi$ with eq. (40) and assuming $A \approx N$ by, at most, $10^{-7}\%$. The agreement is less accurate

Table 1: First row: anomalous perihelion precession, in arcsec cty^{-1} , induced by an uniform and radial acceleration of magnitude $C = 2 \times 10^{-10} \text{ m s}^{-2}$. Second row: estimated corrections $\Delta\dot{\varpi}$, in arcsec cty^{-1} , to the standard Newton/Einstein perihelion precessions of the inner planets according to Table 3 of Ref. [27] (Mercury, Earth, Mars). The result for Venus has been obtained by recently processing radiometric data from Magellan spacecraft (E.V. Pitjeva, private communication, 2008). The reference frame used is a Solar System Barycentric one.

Mercury	Venus	Earth	Mars
2.6611	3.7170	4.3700	5.3714
-0.0036 ± 0.0050	-0.0004 ± 0.0005	-0.0002 ± 0.0004	0.0001 ± 0.0005

for the case $N/E \ll 1$; however, for $a = 100 \text{ kAU}$ the discrepancy turns out to be less than 1% only.

The “standard” form of eq. (5) for μ , plugged into eq. (38), yields, for $E = A_0$,

$$\left(1 + \frac{A}{E}\right) A = N \sqrt{1 + \left(1 + \frac{A}{E}\right)^2}. \quad (54)$$

Let us consider the following limiting cases

- If $A \ll A_0 = E$, as in the Oort cloud, by neglecting terms of order $\mathcal{O}((A/E)^2)$ eq. (54) reduces to

$$A \approx \sqrt{2}N \sqrt{1 + \frac{A}{E}} \approx \sqrt{2}N \left(1 + \frac{A}{2E}\right). \quad (55)$$

Thus, since $N \ll E$,

$$A \approx \frac{\sqrt{2}N}{\left(1 - \frac{N}{\sqrt{2}E}\right)} \approx \sqrt{2}N \left(1 + \frac{N}{\sqrt{2}E}\right) \approx \sqrt{2}N. \quad (56)$$

It can be shown that the same approximated result can be obtained by retaining A/E in the left-hand-side of eq. (54). Also in this case, the internal acceleration of the system becomes quasi-Newtonian.

- For $N \gg A_0 = E$, since $A \approx N + \delta A_0$, $\delta \lesssim A_0$, we can neglect the terms of order of unity with respect to $(A/E)^n$, $n \geq 1$. Thus, eq. (54)

becomes

$$A + E = N\sqrt{1 + \frac{2E}{A}} \approx N\left(1 + \frac{E}{A}\right). \quad (57)$$

It yields

$$A \approx \frac{(N - E) + \sqrt{(E - N)^2 + 4NE}}{2}. \quad (58)$$

which reduces to

$$A \approx \frac{N}{2} \left(1 + \sqrt{1 + \frac{4E}{N}}\right) \approx N + E; \quad (59)$$

it tends to E for $r \rightarrow \infty$ and agrees with eq. (50) obtained with eq. (4). The considerations concerning eq. (51) hold also in this case.

It turns out that approximating X with $(A + E)/A_0$ yields a maximum discrepancy with respect to $|\mathbf{A} + \mathbf{E}|/A_0$ plotted as a function of $0 \leq \alpha \leq 2\pi$ of 0.003% in the planetary region, while at heliocentric distances of 100 kAU the maximum discrepancy is at most 0.2%.

The apparently puzzling situation outlined here can be resolved noting that an EFE numerically equal to A_0 occurs when the planetary motion is referred to a Galactocentric reference frame; indeed, in this case the only external acceleration is due to the gravitational attraction of the Galaxy (and, in principle, to the galaxy M31 Andromeda, other large-scale structures, etc. However, their action is about $0.01 A_0$ [42]), as shown by Figure 13. It seems that the analysis of the Oort cloud by Milgrom in Ref. [38] is based on such a Galactocentric point of view; note that if one considers eq. (47) (and eq. (56)) as describing the Galactocentric motion of an Oort object, by subtracting $\mathbf{A}_\odot = \mathbf{E}$ from it one gets the Oort object-Sun relative motion as difference of their Galactocentric accelerations

$$\mathbf{A}_{\text{rel}} \equiv \mathbf{A} - \mathbf{A}_\odot \approx 2\mathbf{N} - \mathbf{E} \approx -\mathbf{E}. \quad (60)$$

In fact, also \mathbf{E} should be considered as MONDian modified; in the case $E \approx A_0$ this would yield a multiplicative factor of the order of just 1.4 – 2.

Instead, for the internal dynamics of the Solar System, and for a confrontation with the observations and quantities estimated by them like $\Delta\dot{\omega}$, a Solar System Barycenter (SSB) frame must be considered; for practical purposes we will locate the barycenter in the Sun, i.e. we will consider the Sun at rest. In this case, EFE is given by the tidal acceleration \mathbf{T} which is the combination of the uniform centrifugal acceleration \mathbf{C} due to

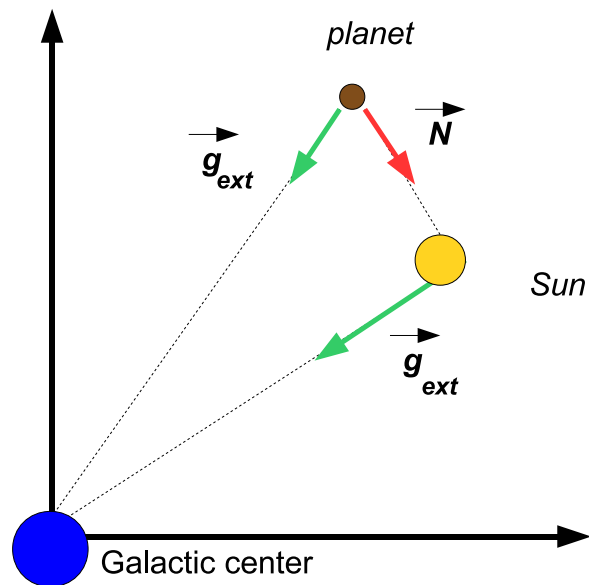


Figure 13: Sun-planet system s embedded in an external system S given by the Milky Way: Galactocentric frame. In it \mathbf{N} (red arrow) is the Newtonian gravitational attraction of the planet by the Sun (the Newtonian gravitational attraction of the Sun by the planet is not depicted), while $\mathbf{E} \equiv \mathbf{g}_{\text{ext}}$ (light green arrow) is the (modified) gravitational attraction of the planet by the Galaxy whose magnitude amounts to about $E \approx 1.8 \times 10^{-10}/\mu \text{ m s}^{-2} \approx 3 \times 10^{-10} \text{ m s}^{-2}$ (in principle, it should also account for the gravitational attraction by other sources external to the Galaxy itself as the galaxy M31 Andromeda, etc.: however, their acceleration is of the order of $\approx 0.01A_0$).

the overall Galactic motion of the Solar System as a whole and the generally non-uniform gravitational attraction by the Galaxy, as shown by Figure 14. Recall that the Sun and planet describe uniform circular motions with radius equal to the Sun-Galactic center distance and centers displaced by an amount equal to the Sun-planet distance, so that they share the same centrifugal accelerations. Since the magnitude of the tidal acceleration is roughly $T \lesssim 10^{-14} \text{ m s}^{-2}$ throughout the Solar System up to the Oort cloud ($30 \text{ kAU} \lesssim r \lesssim 100 \text{ kAU}$), it can certainly be considered as a uniform field over the relatively small extension of the planetary region of the Solar System, contrary to the case of the relatively wide Oort region. In this case, since $T = E \ll A_0$, $T = E \ll N$, eq. (42) reduces to

$$A = \frac{N}{2} \left[1 + \sqrt{1 + \frac{4A_0}{N}} \right], \quad (61)$$

while eq. (38) and eq. (5) yield

$$A = N \sqrt{\frac{1}{2} + \frac{1}{2} \sqrt{1 + \left(\frac{2A_0}{N} \right)^2}}. \quad (62)$$

In this case, eq. (61) and eq. (62) are to be considered as the heliocentric motion of a test particle; note that, for $N \leq A_0$, as in the Oort cloud, they can be approximated as

$$A \approx \frac{N}{2} \left[1 + 2\sqrt{\frac{A_0}{N}} \right], \quad (63)$$

and

$$A \approx \frac{N}{\sqrt{2}} \sqrt{1 + \frac{2A_0}{N}}, \quad (64)$$

yielding a different result with respect to the difference of the Galactocentric accelerations of an Oort object and the Sun by eq. (60). However, let us note that it is difficult to believe that eq. (60) can really describe the Sun-Oort object relative motion since it would yield an almost rectilinear, escaping motion, as a straightforward numerical integration shows for a particle with initial conditions corresponding to semimajor axis $a = 87 \text{ kAU}$, inclination to the ecliptic $i = 134 \text{ deg}$ and eccentricity $e = 0.82$.

In conclusion, claiming that $E = C \approx A_0$ for the internal dynamics Solar System, referred to the usual SSB frame, is erroneous and yield results contradicted by the observations.

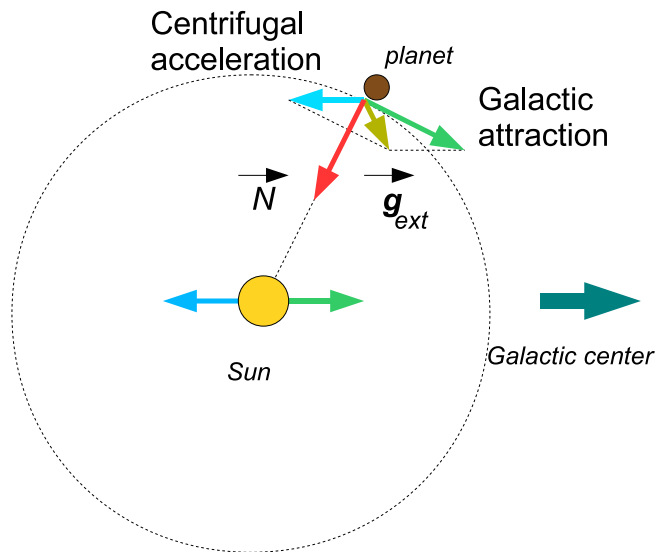


Figure 14: Sun-planet system s embedded in an external system S given by the Milky Way: heliocentric frame. In it \mathbf{N} is the Newtonian gravitational attraction of the planet by the Sun (red arrow), while $\mathbf{E} \equiv \mathbf{g}_{\text{ext}}$ is given by the gravitational tidal forces (olive green arrow) exerted on the planet by the Galaxy whose magnitude amounts to about $E \lesssim 10^{-14} \text{ m s}^{-2}$; they account for both the uniform centrifugal accelerations due to the motion of Solar System through the Galaxy (light blue arrow) and the non-uniform gravitational attraction by the Galaxy throughout the extension of the Solar System (light green arrow).

Acknowledgments

I thank P. Salucci for having strongly encouraged me to rewrite the paper focussing on the Solar System.

References

- [1] A. Bosma, “21-cm line studies of spiral galaxies. I - Observations of the galaxies NGC 5033, 3198, 5055, 2841, and 7331. II - The distribution and kinematics of neutral hydrogen in spiral galaxies of various morphological types”, *The Astronomical Journal*, vol. 86, December 1981, pp. 1791-1846, 1981.
- [2] V. C. Rubin, W. K. Ford, N. Thonnard, and D. Burstein, “Rotational properties of 23 SB galaxies”, *The Astrophysical Journal*, vol. 261, October 15, pp. 439-456, 1982.
- [3] V. C. Rubin, “The Rotation of Spiral Galaxies”, *Science*, vol. 220, no. 4604, pp. 1339-1344, 1983.
- [4] M. Milgrom, “A Modification of the Newtonian Dynamics as a Possible Alternative to the Hidden Mass Hypothesis”, *The Astrophysical Journal*, vol. 270, July 15, pp. 365-370, 1983a.
- [5] M. Milgrom, “A Modification of the Newtonian Dynamics - Implications for Galaxies”, *The Astrophysical Journal*, vol. 270, July 15, pp. 371-389, 1983b.
- [6] M. Milgrom, “A Modification of the Newtonian Dynamics - Implications for Galaxy Systems”, *The Astrophysical Journal*, vol. 270, July 15, pp. 384-389, 1983c.
- [7] K. G. Begeman, A. H. Broeils, and R. H. Sanders, “Extended rotation curves of spiral galaxies - Dark haloes and modified dynamics”, *Monthly Notices of the Royal Astronomical Society*, vol. 249, April 1, pp. 523-537, 1991.
- [8] B. Famaey, and J. Binney, “Modified Newtonian dynamics in the Milky Way”, *Monthly Notices of the Royal Astronomical Society*, vol. 363, no. 2, pp. 603-608, 2005.

- [9] J. D. Bekenstein, and M. Milgrom, “Does the Missing Mass Problem Signal the Breakdown of Newtonian Gravity?”, *The Astrophysical Journal*, vol. 286, November 1, pp. 7-14, 1984.
- [10] H. Zhao, and B. Famaey, “Refining the MOND Interpolating Function and TeVeS Lagrangian”, *The Astrophysical Journal*, vol. 638, no. 1, pp. L9-L12, 2006.
- [11] B. Famaey, G. Gentile, J.-P. Bruneton, and H. Zhao, “Insight into the baryon-gravity relation in galaxies”, *Physical Review D*, vol. 75, no. 6, id. 063002, 2007.
- [12] R. H. Sanders, and E. Noordermeer, “Confrontation of Modified Newtonian Dynamics with the rotation curves of early-type disc galaxies”, *Monthly Notices of the Royal Astronomical Society*, vol. 379, no. 2, pp. 702-710, 2007.
- [13] R. Brada, and M. Milgrom, “Exact solutions and approximations of MOND fields of disc galaxies”, *Monthly Notices of the Royal Astronomical Society*, vol. 276, no. 2, pp. 453-459, 1995.
- [14] J. D. Bekenstein, “Relativistic gravitation theory for the modified Newtonian dynamics paradigm”, *Physical Review D*, vol. 70, no. 8, id. 083509, 2004.
- [15] J.-P. Bruneton, and G. Esposito-Farèse, “Field-theoretical formulations of MOND-like gravity”, *Physical Review D*, vol. 76, no. 12, id. 124012, 2007.
- [16] H. Zhao, “Coincidences of Dark Energy with Dark Matter: Clues for a Simple Alternative?”, *The Astrophysical Journal*, vol. 671, no. 1, pp. L1-L4, 2007.
- [17] R. H. Sanders, and S. S. McGaugh, “Modified Newtonian Dynamics as an Alternative to Dark Matter”, *Annual Review of Astronomy and Astrophysics*, vol. 40, September 2002, pp. 263-317, 2002.
- [18] J. D. Bekenstein, “The modified Newtonian dynamics - MOND and its implications for new physics”, *Contemporary Physics*, vol. 47, no. 6, pp. 387-403, 2006.
- [19] M. Milgrom, “The MOND paradigm”, Talk presented at the XIX Rencontres de Blois “Matter and energy in the Universe: from nucleosynthesis to cosmology”, May 2007, <http://arxiv.org/abs/0801.3133v2>.

- [20] J. H. Oort, “The structure of the cloud of comets surrounding the Solar System and a hypothesis concerning its origin”, *Bullettin of the Astronomical Institutes of The Netherlands*, vol. 11, no. 408, pp. 91-110, 1950.
- [21] M. Milgrom, “Solutions for the modified Newtonian dynamics field equation”, *The Astrophysical Journal*, vol. 302, March 15, pp. 617-625, 1986.
- [22] C. Talmadge, J.-P. Berthias, R. W. Hellings, and E. M. Standish, “Model-independent constraints on possible modifications of Newtonian gravity”, *Physical Review Letters*, vol. 61, no. 10, pp. 1159-1162, 1988.
- [23] M. Sereno, and Ph. Jetzer, “Dark matter versus modifications of the gravitational inverse-square law: results from planetary motion in the Solar system”, *Monthly Notices of the Royal Astronomical Society*, vol. 371, no. 2, pp. 626-632, 2006.
- [24] J. D. Bekenstein, and J. Magueijo, “Modified Newtonian dynamics habitats within the solar system”, *Physical Review D*, vol. 73, no. 10, id. 103513, 2006.
- [25] R. H. Sanders, “Solar system constraints on multifield theories of modified dynamics”, *Monthly Notices of the Royal Astronomical Society*, vol. 370, no. 3, pp. 1519-1528, 2006.
- [26] L. Iorio, “Constraining MOND with Solar System dynamics”, *Journal of Gravitational Physics*, vol. 2, no. 1, pp. 26-32, 2008.
- [27] E. V. Pitjeva, “Relativistic Effects and Solar Oblateness from Radar Observations of Planets and Spacecraft”, *Astronomy Letters*, vol. 31, no. 5, pp. 340-349, 2005.
- [28] I. I. Shapiro, in: H. Woolf (ed.), *Some Strangeness in the. Proportion*, Addison-Wesley, Reading, Mass., 1980.
- [29] A. Moribidelli, “Origin and Dynamical Evolution of Comets and their Reservoirs”, <http://arxiv.org/abs/astro-ph/0512256>, 2005.
- [30] J., Heisler, S. Tremaine, and C. Alcock, “The frequency and intensity of comet showers from the Oort cloud”, *Icarus*, vol. 70, no. 2, pp. 269-288, 1987.

- [31] J. J. Matese, P. G. Whitman, K. A. Innanen, and M. J. Valtonen, “Periodic Modulation of the Oort Cloud Comet Flux by the Adiabatically Changing Galactic Tide”, *Icarus*, vol. 116, no. 2, pp. 255-268, 1995.
- [32] M. Fouchard, C. Froeschlé, G. Valsecchi, and H. Rickman, “Long-term effects of the Galactic tide on cometary dynamics”, *Celestial Mechanics and Dynamical Astronomy*, vol. 95, no. 1-4, pp. 299-326, 2006.
- [33] B. Famaey, *Kynematics and Dynamics of Giant Stars in the Solar Neighbourhood*, *PhD Thesis*, Universite Libre de Bruxelles, Faculté des Sciences, 2003.
- [34] E. V. Pitjeva, “Use of optical and radio astrometric observations of planets, satellites and spacecraft for ephemeris astronomy” in: W. J. Jin, I. Platais, and M. A. C. Perryman (eds.), *A Giant Step: from Milli- to Micro-arcsecond Astrometry, Proceedings of the International Astronomical Union, IAU Symposium, Volume 248*, pp. 20-22, 2008.
- [35] W. M. Folkner, E. M. Standish, J. G. Williams, and D. H. Boggs. “Planetary and lunar ephemeris DE418”, *Interoffice Memorandum IOM 343R-07-005*, 2008. (<ftp://ssd.jpl.nasa.gov/pub/eph/planets/ioms/>)
- [36] A. Fienga, H. Manche, J. Laskar, and M. Gastineau, “INPOP06: a new numerical planetary ephemeris”, *Astronomy and Astrophysics*, vol. 477, no. 1, pp. 315327, 2008.
- [37] E. M. Standish jr., “JPL Planetary and Lunar Ephemerides, DE414”, *Interoffice Memorandum IOM 343R-06-002*, 2006.
- [38] M. Milgrom, “Solutions for the modified Newtonian dynamics field equation”, *The Astrophysical Journal*, vol. 302, march 15, pp. 617-625, 1986.
- [39] B. Famaey, J.-P. Bruneton, and H.-S. Zhao, “Escaping from modified Newtonian dynamics”, *Monthly Notices of the Royal Astronomical Society: Letters*, vol. 377, no. 1, pp. L79-L82, 2007.
- [40] G. Angus, and S. McGaugh, “The collision velocity of the bullet cluster in conventional and modified dynamics”, *Monthly Notices of the Royal Astronomical Society*, vol. 383, no. 2, pp. 417-423, 2008.
- [41] R. Brada, and M. Milgrom, “The Modified Newtonian Dynamics Predicts an Absolute Maximum to the Acceleration Produced by “Dark Halos””, *The Astrophysical Journal*, vol. 512, no. 1, pp. L17-L18, 1999.

- [42] X. Wu, B. Famaey, G. Gentile, H. Perets, and H. Zhao, “Milky Way potentials in CCDMMOND. Is the Large Magellanic Cloud on a bound orbit?”, *Monthly Notices of the Royal Astronomical Society*, vol. 386, no. 4, pp. 2199-2208, 2008.
- [43] L. Iorio, and G. Giudice, “What do the orbital motions of the outer planets of the Solar System tell us about the Pioneer anomaly?”, *New Astronomy*, vol. 11, no. 8, pp. 600-607, 2006.